



Castellani, M., Lemmens, Y., & Cooper, J. (2016). Parametric reduced-order model approach for simulation and optimization of aeroelastic systems with structural nonlinearities. *Proceedings of the Institution of Mechanical Engineers, Part G: Journal of Aerospace Engineering*, 230(8), 1359-1370. DOI: 10.1177/0954410015608888

Peer reviewed version

Link to published version (if available):  
[10.1177/0954410015608888](https://doi.org/10.1177/0954410015608888)

[Link to publication record in Explore Bristol Research](#)  
PDF-document

This is the author accepted manuscript (AAM). The final published version (version of record) is available online via Sage at <http://pig.sagepub.com/content/230/8/1359>. Please refer to any applicable terms of use of the publisher.

## University of Bristol - Explore Bristol Research

### General rights

This document is made available in accordance with publisher policies. Please cite only the published version using the reference above. Full terms of use are available:  
<http://www.bristol.ac.uk/pure/about/ebr-terms.html>

# **Parametric reduced order model approach for simulation and optimization of aeroelastic systems with structural nonlinearities**

Michele Castellani<sup>1,2</sup>, Yves Lemmens<sup>1</sup> and Jonathan E Cooper<sup>2</sup>

<sup>1</sup>Aerospace Centre of Competence, Siemens PLM Software, Belgium

<sup>2</sup>Department of Aerospace Engineering, Faculty of Engineering, University of Bristol, UK

## **Corresponding author:**

Michele Castellani, Aerospace Centre of Competence, Siemens PLM Software (Belgium), Interleuvenlaan 68, 3001 Leuven, Belgium

Email: michele.castellani@siemens.com

## **Abstract**

A method based on Parametric Reduced Order Models to efficiently predict the transient response of aeroelastic systems with concentrated structural nonlinearities is presented. The approach approximates the nonlinear response in a piecewise-linear manner through time integration of sub-linear reduced order models; these are parameterized with respect to the nonlinearity and are efficiently obtained by balanced truncation and interpolation. The procedure is applied to the optimization of a wing tip device for passive loads alleviation which features a nonlinear stiffness, showing the effectiveness and efficiency of the methodology.

## **Keywords**

Aircraft loads, aeroelastic response, structural nonlinearities, load alleviation, adaptive wing tip, Parametric ROM

## **Introduction**

Aeroelastic analyses of aircraft have been traditionally performed under the assumption of linear aerodynamics and structure. The industrial practice still heavily relies upon the linear approach, nevertheless it is recognized that many

aeroelastic phenomena cannot be predicted without considering nonlinear effects that can arise from the aerodynamic flowfield, the structure or the flight control system<sup>1,2</sup>.

Structural nonlinearities can be classified as being either distributed or concentrated; the former are due to material or geometric nonlinearities of the structure, whereas the latter stem from freeplay, hysteresis, friction or nonlinear force-displacement relationships in control surfaces, linkages or connections between wing, pylons, engine or stores<sup>2,3,4</sup>. Most of the studies on concentrated structural nonlinearities have dealt with predicting Limit Cycle Oscillations (LCOs)<sup>3,4,5,6,7</sup>. On the other hand, there has been less focus on the impact of structural nonlinearities on aircraft loads. The certification specifications for large civil transport aircraft, EASA CS-25 AMC Subpart-C.8<sup>8,9</sup>, explicitly require to realistically or conservatively represent in loads calculation any structural, aerodynamic or system characteristic which may cause the aircraft response to become nonlinear. When an explicit simulation of nonlinearities is required, it is suggested to calculate loads through time-domain integration of the equations of motion. Typically however, a linear structural model is used for loads prediction as the nonlinear characteristics of the airframe are minor and it is an acceptable conservative assumption<sup>8</sup>.

This paper presents an efficient methodology for predicting the aeroelastic response of systems with concentrated structural nonlinearities, focusing on gust loads calculation. The procedure follows the time-domain integration approach and approximates the nonlinear response as a series of piecewise-linear subsystems, updated at each time step based on the current configuration of the system. In this way, a generic concentrated nonlinearity can be straightforwardly introduced into the classical linear models that are still routinely employed in the practice, without the need of resorting to full nonlinear aeroelastic solutions not readily available. Similar methods have been proposed in the electrical engineering field<sup>10</sup> and for multibody dynamics<sup>11</sup>. In aeroelasticity, Chen et al.<sup>12</sup> have presented a method based on the integration of discrete linear state-space models and applied it to study the aeroelastic stability of an airfoil with freeplay and of a joined wing aircraft subject to buckling

The proposed procedure is based upon Parametric Model Order Reduction (PMOR)<sup>13</sup> and it aims at reducing significantly the computational effort associated to the time simulations by employing reduced order piecewise-linear models which are parameterized with respect to the nonlinear property and efficiently obtained combining Model Order Reduction and interpolation of the parametric models. The methodology is applied to the optimization of a passive wing tip device for load alleviation featuring a nonlinear stiffness, which was first presented by Ricci et al.<sup>14</sup>.

### Aeroelastic systems with concentrated structural nonlinearities

Aeroelastic analyses are typically performed in the frequency-domain. This approach is computationally efficient and simplifies the analysis procedure; however, it is not suitable for the transient response of aeroelastic systems when nonlinearities, being structural, aerodynamic or in the flight control systems, are involved. In this latter case a time-domain simulation is required. The trade-off is a higher computational time and complexity, but any kind of nonlinearities can be included.

The linear aeroelastic equations of motion in time-domain, assuming a FE discretization of the structure, can be written as

$$\mathbf{M}_{aa}\ddot{\mathbf{u}}_a + \mathbf{C}_{aa}\dot{\mathbf{u}}_a + \mathbf{K}_{aa}\mathbf{u}_a = q_\infty \mathbf{Q}_{aa}\mathbf{u}_a + q_\infty \mathbf{F}_{ag} \quad (1)$$

where  $\mathbf{M}_{aa}$ ,  $\mathbf{C}_{aa}$  and  $\mathbf{K}_{aa}$  are respectively the mass, damping and stiffness matrices,  $\mathbf{u}_a$  the vector of the displacements,  $q_\infty$  the dynamic pressure,  $\mathbf{Q}_{aa}$  the matrix of the unsteady aerodynamics forces due to the structural motion and  $\mathbf{F}_{ag}$  the vector of the unsteady aerodynamic forces due to a gust. Typically equation (1) is expressed in generalized coordinates  $\mathbf{q}_h$  to reduce the size of the problem. A common choice for the generalized basis is a set of the low frequency normal modes of the structure  $\Phi_{ah}$ , leading to

$$\mathbf{M}_{hh}\ddot{\mathbf{q}}_h + \mathbf{C}_{hh}\dot{\mathbf{q}}_h + \mathbf{K}_{hh}\mathbf{q}_h = q_\infty \mathbf{Q}_{hh}\mathbf{q}_h + q_\infty \mathbf{Q}_{hg} \quad (2)$$

In this work the generalized unsteady aerodynamic forces (GAF) are calculated by the Doublet Lattice Method<sup>15</sup> (DLM) and thus are available in the frequency-domain as complex matrices tabulated for a set of reduced frequencies and a fixed Mach number. To cast the equations in time-domain, a Rational Function Approximation of  $\mathbf{Q}_{hh}$  and  $\mathbf{Q}_{hg}$  is performed using Roger's method<sup>16</sup>, that is

$$\tilde{\mathbf{Q}}_{hh}(s) = \mathbf{D}_0 + \frac{l_a}{u_\infty} \mathbf{D}_1 s + \left(\frac{l_a}{u_\infty}\right)^2 \mathbf{D}_2 s^2 + \frac{u_\infty}{l_a} \sum_{l=1}^{n_a} \frac{s}{s + u_\infty/l_a \beta_l} \mathbf{A}_l \quad (3)$$

$$\tilde{\mathbf{Q}}_{hg}(s) = \mathbf{D}_{0g} + \frac{l_a}{u_\infty} \mathbf{D}_{1g} s + \left(\frac{l_a}{u_\infty}\right)^2 \mathbf{D}_{2g} s^2 + \frac{u_\infty}{l_a} \sum_{l=1}^{n_g} \frac{s}{s + u_\infty/l_a \beta_{g,l}} \mathbf{A}_{g,l} \quad (4)$$

where  $s$  is the Laplace variable,  $l_a$  a reference length and the coefficients of the matrices are calculated by a least-square fit. The original formulation by Roger is extended considering the  $n_a$  aerodynamic poles  $\beta_l$  due to the structural motion and the  $n_g$  gust aerodynamic poles  $\beta_{g,l}$  as free design variables of an optimization process, whose objective function is the minimization of the squared error between the approximated and tabulated GAF, and subject to the constraint of asymptotic stability of the aerodynamic poles, i.e.  $\beta_l < 0$  and  $\beta_{g,l} < 0$ . The whole RFA procedure consists therefore of a two-level optimization: an inner linear least-square curve fitting for the coefficients matrices at the numerator of equations (3) and (4) and an outer nonlinear constrained optimization, via a genetic algorithm, for the aerodynamic poles. Two separate RFAs are performed on  $\mathbf{Q}_{hh}$  and on  $\mathbf{Q}_{hg}$ , imposing the matching of the generalized forces at  $k = 0$  and assuming respectively 5 and 6 aerodynamic poles. This approach allows for a greater flexibility in the selection of the poles and increases the fitting accuracy of both terms.

Eventually, the aeroelastic system in time-domain is obtained and formulated as a state-space Linear Time Invariant (LTI) system

$$\dot{\mathbf{x}}_{ae} = \mathbf{A}_{ae}\mathbf{x}_{ae} + \mathbf{B}_{ae}\mathbf{u} \quad (5)$$

$$\mathbf{y} = \mathbf{C}_{ae}\mathbf{x}_{ae} + \mathbf{D}_{ae}\mathbf{u} \quad (6)$$

The states vector  $\mathbf{x}_{ae}$  includes the generalized coordinates, their time derivatives and the aerodynamic states of the structural and gust GAFs. The input  $\mathbf{u}$  is a vertical discrete gust and the output vector  $\mathbf{y}$  contains the wing internal loads (shear, bending moment and torque), calculated by mode displacement.

### **Modelling of concentrated nonlinearities**

In industrial practice, aeroelastic analyses are still routinely performed using linear models and tools. Nonlinear aeroelastic solvers are not readily available and the alternative approach is a co-simulation between a nonlinear structural solver and an aerodynamic solver, which leads to a considerable increase in complexity and computational time.

The method proposed in this work considers a linear piecewise discretization of the arbitrary nonlinearity based on the current configuration of the system throughout the transient response. In this way, a nonlinear system is simulated as a series of piecewise LTI systems that can be generated with standard aeroelastic tools.

Considering, without loss of generality, a cubic nonlinear force-displacement relationship of a flexible element of the FE model of the structure, a linearized equivalent stiffness can be computed as

$$\mathbf{K}(\boldsymbol{\theta}(t)) = \mathbf{K}_0 + \mathbf{K}_{nl}\boldsymbol{\theta}^2(t) \quad (7)$$

where  $K_0$  is the linear part of the stiffness and  $\theta$  the Degree Of Freedom (DOF) where the nonlinearity acts. During the nonlinear response, changes in stiffness occur based on the actual value of  $\theta$ . In a linearized fashion, these can be represented as an incremental stiffness matrix  $\Delta\mathbf{K}_{aa}$  to be added to the stiffness matrix of the linear model  $\mathbf{K}_{0,aa}$  at each time step based on the current deflection  $\bar{\theta}$ . The actual generalized stiffness is then given by

$$\mathbf{K}_{hh}(\bar{\theta}) = \boldsymbol{\Phi}_{ah}^T [\mathbf{K}_{0,aa} + \Delta\mathbf{K}_{aa}(\bar{\theta})] \boldsymbol{\Phi}_{ah} \quad (8)$$

Thus the nonlinear system is approximated by a collection of linearized LTI systems parameterized by the nonlinear physical DOF  $\theta$

$$\dot{\mathbf{x}}_{ae}(\boldsymbol{\theta}) = \mathbf{A}_{ae}(\boldsymbol{\theta})\mathbf{x}_{ae}(\boldsymbol{\theta}) + \mathbf{B}_{ae}(\boldsymbol{\theta})\mathbf{u} \quad (9)$$

$$\mathbf{y}(\boldsymbol{\theta}) = \mathbf{C}_{ae}(\boldsymbol{\theta})\mathbf{x}_{ae}(\boldsymbol{\theta}) + \mathbf{D}_{ae}(\boldsymbol{\theta})\mathbf{u} \quad (10)$$

### Generalized basis with structural nonlinearities

An issue for aeroelastic systems with structural nonlinearities is the choice of an adequate generalized basis. A unique set of normal modes does not strictly exist anymore, but it changes according to the configuration of the structure. For this reason, it is necessary to select a unique generalized basis capable of representing the physical displacements in the entire domain of the nonlinear response.

A number of methods have been proposed for this purpose: component mode synthesis<sup>17</sup>, fictitious mass<sup>18</sup>, residual vectors<sup>19,20</sup>. In this work, the residual vectors method is applied which consists of adding to the normal modes of a baseline configuration (for the nonlinear case assumed to be the undeformed aircraft) shape vectors corresponding to a unit displacement (or rotation) of the DOF where the nonlinearity is located, computed by static solution. A

reorthogonalization of the augmented basis to the baseline mass and stiffness matrices is performed to remove redundant components and obtain a basis which diagonalizes the baseline mass and stiffness matrices.

The addition of the residual vectors to the normal modes produces high frequency synthetic modes representing the local deformation in the proximity of the DOFs of interest. The static participation of these shapes is paramount in achieving accuracy whereas the dynamic response could generate spurious oscillations that do not represent the physical response of the structure. To overcome this pitfall, critical damping is assigned to these synthetic modes.

### **Parametric Model Order Reduction for aeroelastic systems with concentrated structural nonlinearities**

The size of the aeroelastic system in state-space form, though being already reduced from physical to generalized coordinates, can still be relatively high when used for aircraft loads calculation, where thousands of load cases must be analysed, and even more if nonlinearities are present and a dedicated solution procedure is carried out.

The system of equations (9) is a function of the DOF  $\theta$ ; besides, the equations depend also on the flight condition, i.e. altitude and Mach number, that has to be varied to cover the whole flight envelope as required by the certification authorities. Therefore the solution needs to be computed over a potentially large range of parameter values.

A significant saving in computational time is possible if, instead of the original Full Order Model (FOM) of equation (9), a Reduced Order Model (ROM) is used which is able to retain the accuracy and preserve the parametric dependency over a broad range of parameters. The generation of a new ROM at each point of interest in the parameter space is in fact usually impractical and could even be more computationally expensive than building and evaluating the FOM anew. To overcome this issue, Parametric Model Order Reduction has been introduced to efficiently generate Parametric ROMs (PROMs), without the need of performing a new reduction at each design point. A survey of the state-of-the-art in PMOR is given by Benner et al.<sup>13</sup>.

To present the methodology applied in this work, the LTI aeroelastic system, of order  $N$ , is considered in the form

$$\dot{\mathbf{x}}_{ae}(\mathbf{p}, \boldsymbol{\theta}) = \mathbf{A}_{ae}(\mathbf{p}, \boldsymbol{\theta})\mathbf{x}_{ae}(\mathbf{p}, \boldsymbol{\theta}) + \mathbf{B}_{ae}(\mathbf{p}, \boldsymbol{\theta})\mathbf{u} \quad (11)$$

$$\mathbf{y}(\mathbf{p}, \boldsymbol{\theta}) = \mathbf{C}_{ae}(\mathbf{p}, \boldsymbol{\theta})\mathbf{x}_{ae}(\mathbf{p}, \boldsymbol{\theta}) + \mathbf{D}_{ae}(\mathbf{p}, \boldsymbol{\theta})\mathbf{u} \quad (12)$$

where  $\theta$  is the physical DOF where a concentrated structural nonlinearity acts and  $\mathbf{p} \in \mathbb{R}^d$  is a set of parameters on which the state-space matrices arbitrarily depend, in this specific work altitude and Mach number. A projection-based reduction by balanced truncation<sup>21</sup> is applied to generate a ROM of order  $n_r \ll N$

$$\dot{\mathbf{x}}_r(\mathbf{p}, \theta) = \mathbf{A}_r(\mathbf{p}, \theta)\mathbf{x}_r(\mathbf{p}, \theta) + \mathbf{B}_r(\mathbf{p}, \theta)\mathbf{u} \quad (13)$$

$$\mathbf{y}_r(\mathbf{p}, \theta) = \mathbf{C}_r(\mathbf{p}, \theta)\mathbf{x}_r(\mathbf{p}, \theta) + \mathbf{D}_r(\mathbf{p}, \theta)\mathbf{u} \quad (14)$$

where the Reduced Order Basis (ROB) is  $\mathbf{T}_B \in \mathbb{R}^{N \times n_r}$  and the reduced order matrices are

$$\mathbf{A}_r = \mathbf{T}_B \mathbf{A} \mathbf{T}_B^{-1} \quad (15)$$

$$\mathbf{B}_r = \mathbf{T}_B \mathbf{B} \quad (16)$$

$$\mathbf{C}_r = \mathbf{C} \mathbf{T}_B^{-1} \quad (17)$$

Balanced truncation is one of the most common order reduction techniques employed in the control system fields and has desirable properties such as stability preservation of the reduced models and an  $H_\infty$  error bound. Moreover, the dimension of the ROM can be selected by checking the decay of the Hankel singular values of the state-space system in balanced form.

To obtain a ROM that can retain the parametric dependency various strategies have been proposed<sup>13</sup>. The procedure applied herein is based on the construction of a database of ROMs at few selected sampling points  $(\hat{\mathbf{p}}_i, \hat{\theta}_j)$  in the parameter domain and by interpolation of the reduced state-space matrices at all the other points of interest for the simulation  $(\bar{\mathbf{p}}_r, \bar{\theta}_s)$ . This method has been successfully applied in the past in aeroelasticity, for fast flutter clearance of a wing-store configuration<sup>22</sup>, in control system design of a flexible aircraft<sup>23</sup> and unsteady CFD<sup>24</sup>. This paper presents its extension to the transient response and loads prediction of aeroelastic systems with concentrated structural nonlinearities and its application in an optimization framework.

The PMOR framework proposed by Panzer et al.<sup>25</sup> is followed. It consists of the following steps:

1. Generation of the  $k = 1 \dots n_p \times n_\theta$  local ROMs at the sampling points  $\hat{\mathbf{p}}_i, i = 1 \dots n_p$  and  $\hat{\theta}_j, j = 1 \dots n_\theta$
2. Congruence transformation of the locally reduced state-space matrices



3. Elementwise interpolation of the locally reduced state-space matrices to the unsampled points of interest for the analyses  $(\bar{\mathbf{p}}_r, \bar{\theta}_s)$
4. Time simulation of the resulting interpolated ROM.

In the first step, the parameter space is sampled, the FOMs constructed at each of these points and then individually reduced through balanced truncation. All the local ROMs have the same order  $n_r$ .

As the balanced truncation is not a physics-based reduction, such as the modal condensation, but a purely mathematical one, the states of the ROMs at different parameter values lie in unrelated subspaces and, before the interpolation, must be transformed, through a similarity transformation  $\mathbf{x}_{r,k} = \mathbf{P}_k \hat{\mathbf{x}}_{r,k}$ , to a congruent common subspace. For details on this transformation refer to Panzer et al.<sup>25</sup> and Castellani et al.<sup>26</sup>.

The congruence transformed local ROMs are given by

$$\hat{\mathbf{A}}_{r,k} = \mathbf{P}_k^T \mathbf{T}_B \mathbf{A}(\hat{\mathbf{p}}_i, \hat{\theta}_j) \mathbf{T}_{B,k}^{-1} \mathbf{P}_k \quad (18)$$

$$\hat{\mathbf{B}}_{r,k} = \mathbf{P}_k^T \mathbf{T}_B \mathbf{B}(\hat{\mathbf{p}}_i, \hat{\theta}_j) \quad (19)$$

$$\hat{\mathbf{C}}_{r,k} = \mathbf{C}(\hat{\mathbf{p}}_i, \hat{\theta}_j) \mathbf{T}_{B,k}^{-1} \mathbf{P}_k \quad (20)$$

Once all the local reduced models are available in this form, the resulting PROM at  $(\bar{\mathbf{p}}_r, \bar{\theta}_s)$  is obtained by elementwise linear or spline interpolation of the matrices in equations (18) to (20).

#### *Solution procedure for systems with concentrated structural nonlinearities*

The extension of the PMOR methodology, in combination with the previously introduced modelling of concentrated structural nonlinearities, is now presented. In the framework of the approximation of the nonlinear system as a series of piecewise-linear LTI system, the nonlinear property, in this specific case a cubic restoring force in the DOF  $\theta$  of the FE model, is treated as a parameter of the equations that varies throughout the transient response, unlike the altitude and Mach number which are constant once a flight condition is chosen. In place of FOMs, ROMs generated as previously presented are employed.

The matrices of the linear ROMs are not constant anymore throughout the response, but dependant on the actual configuration of the system via the nonlinear property  $K(\theta(t))$ . At each time step  $t_i$  of the integration, an updated

ROM is built by interpolation according to the current value of  $\theta(t_i)$  and used for the next time step. The response of  $\theta$  is calculated from the states of the system and monitored during the simulation.

Thus a nonlinear system is simulated by switching between sub-linear ones. Compared to a fully nonlinear analysis this piecewise-linear approach is, on one hand, an approximation, and on the other, a more computationally efficient way and relies on the standard linear aeroelastic tools.

The workflow of the procedure is depicted in Figure 1 and follows as:

1. A database of linear ROMs is generated in an off-line phase for a discrete set of values of the linearized equivalent stiffness  $\hat{K}_j$  and a fixed flight condition
2. The time integration starts from the initial conditions using a state-transition matrix integration
3. The value of the linearized equivalent stiffness at the current time step  $t_i$  is calculated based on the actual deflection  $\theta(t_i)$ , recovered from the states  $\mathbf{x}_r(t_i)$
4. The updated ROM matrices  $\mathbf{A}_r(\theta(t_i))$ ,  $\mathbf{B}_r(\theta(t_i))$ ,  $\mathbf{C}_r(\theta(t_i))$ ,  $\mathbf{D}_r(\theta(t_i))$  are calculated by interpolation from the database generated off-line at step 1
5. The updated ROM is used for the next integration step  $t_{i+1}$ .

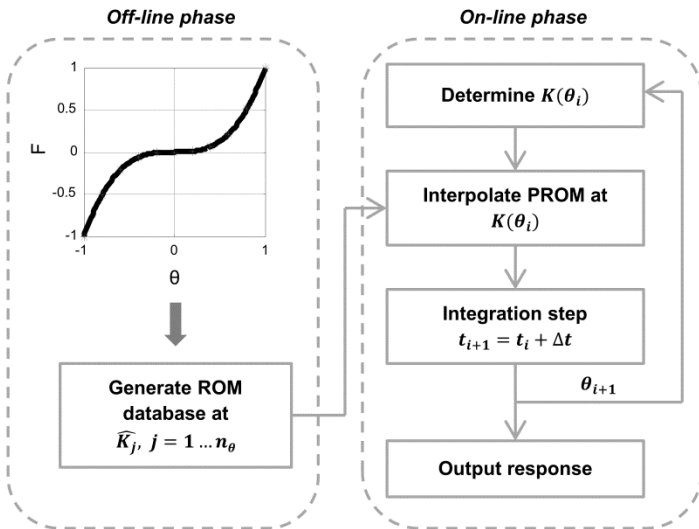


**Figure 1.** Flowchart of the PROM procedure for systems with concentrated structural nonlinearities.

The selection of the sampling points for the linearized equivalent stiffness is critical for the accuracy of the procedure. These must cover the entire expected range of variations during the nonlinear response and must be fine enough to limit the interpolation error.

Since the matrices interpolation and switching is performed at each time step, the number of interpolations can be significantly high. Thus the benefit of using a ROM instead of a FOM is clear, especially when several flight conditions must be analysed for loads prediction or if the nonlinear transient response is used in an optimization.

### Optimization of a nonlinear wing tip device

The PROM approach is applied to the optimization of a nonlinear wing tip device for load alleviation. A preceding publication by one of the authors<sup>14</sup> proposed a wing tip device, shown in Figure 2, with a passive load alleviation capability. The main purpose of this device, attached to the outboard wing, is to extend the wingspan in order to achieve a reduction in induced drag and, eventually, in fuel consumption. This goal conflicts with the increase in loads and, as a result, in structural weight caused by a span extension. A system is devised to embed in the wing tip a passive load alleviation function by connecting it to the outboard wing through a flexible element, located ahead of the wing tip's centre of pressure, whose torsional stiffness is tuned to provide alignment of the wing tip and the main wing in cruise flight and to allow the pitching motion of the wing tip surface, in the direction of a load reduction, at increasing load levels.

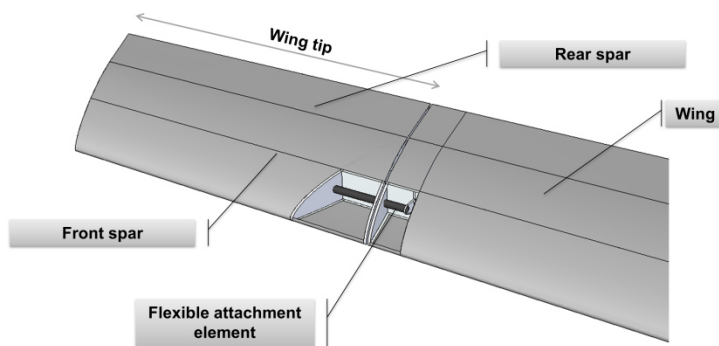


**Figure 2.** Design concept of the wing tip device<sup>14</sup>.

The original design of the wing tip<sup>14</sup> featured a flexible attachment element with a linear stiffness, which was selected to maximize the wing bending moment alleviation, with respect to a rigid wing span extension, via a

constrained gradient-based optimization. In this paper the effect of a nonlinear stiffness of the attachment element on the wing bending moment alleviation is studied applying the PROM procedure proposed. A cubic restoring force of the attachment element in the torsional DOF  $\theta$  is assumed, which leads to the linearized equivalent stiffness of equation (7) such that

$$K(\theta(t)) = K_0 + K_{nl}\theta^2(t)$$

where the two coefficients  $K_0$  and  $K_{nl}$  define respectively the linear and the nonlinear (cubic) contribution to the restoring force.

As shown by Ricci et al.<sup>14</sup> for the linear design, the more flexible is the attachment element the greater is the bending moment alleviation achieved. This however would results in an excessive misalignment of the wing tip in cruise, which could increase the interference drag and drag due to flow separation and offset the reduction in induced drag. A similar study<sup>29</sup> showed that increasing the flexibility of such an attachment also increased the likelihood of flutter occurring.

A multi-objective optimization of the nonlinear stiffness is therefore carried out, assuming as design variables  $K_0$  and  $K_{nl}$ , and two conflicting objective functions are identified:

1. Minimization of worst-case Max/Min wing bending moment along the wingspan with respect to the linear design

$$\mathcal{F}_1 = \mathbf{1}/I_S \sum_{j=1}^{n_{sec}} \left( \left| \frac{BM_{max,j}^{NL}}{BM_{max,j}^{LIN}} \right| + \left| \frac{BM_{min,j}^{NL}}{BM_{min,j}^{LIN}} \right| \right) \quad (21)$$

2. Minimization of the wing tip misalignment  $\theta_{1g,k}$  in cruise condition.

$$\mathcal{F}_2 = \mathbf{1}/M \sum_{k=1}^M \left( \left| \frac{\theta_{1g,k}}{\bar{\theta}_{1g}} \right| \right) \quad (22)$$

where  $BM_{max,j}^{NL}$ ,  $BM_{min,j}^{NL}$  and  $BM_{max,j}^{LIN}$ ,  $BM_{min,j}^{LIN}$  are the maximum and minimum total bending moment of the aircraft respectively with the nonlinear and linear device, due to the gust and the initial 1g trim condition, at the wing section  $j$  among all the flight conditions.  $I_S$  and  $\bar{\theta}_{1g}$  are a normalization factors.

A set of  $M$  flight conditions covering the whole flight envelope and one mass configuration (MZFW) are considered. Trim analyses in cruise condition at 1g, including static aeroelastic effects, and gust responses are performed at all the selected flight conditions. As required by the certification specifications, vertical gusts, both upward and downward, with a “1-cosine” velocity profile and ten evenly spaced gust gradients between 30ft and 350ft are analysed. Gust response has often been chosen as the objective function of aeroelastic optimization<sup>30</sup> since it is usually the critical load case for a modern airliner.

Because the system under consideration is nonlinear, the gust response depends on the initial trim condition and loads due to the gust and to cruise flight cannot be calculated independently and superimposed as done in linear analysis. Therefore, in the optimization process for each flight condition a nonlinear trim analysis is first performed to calculate the initial wing tip relative deflection and wing loads and then this solution is used as the initial condition for the time integration procedure of the nonlinear gust response.

The entire procedure for the optimization using the PROM is shown in Figure 3.

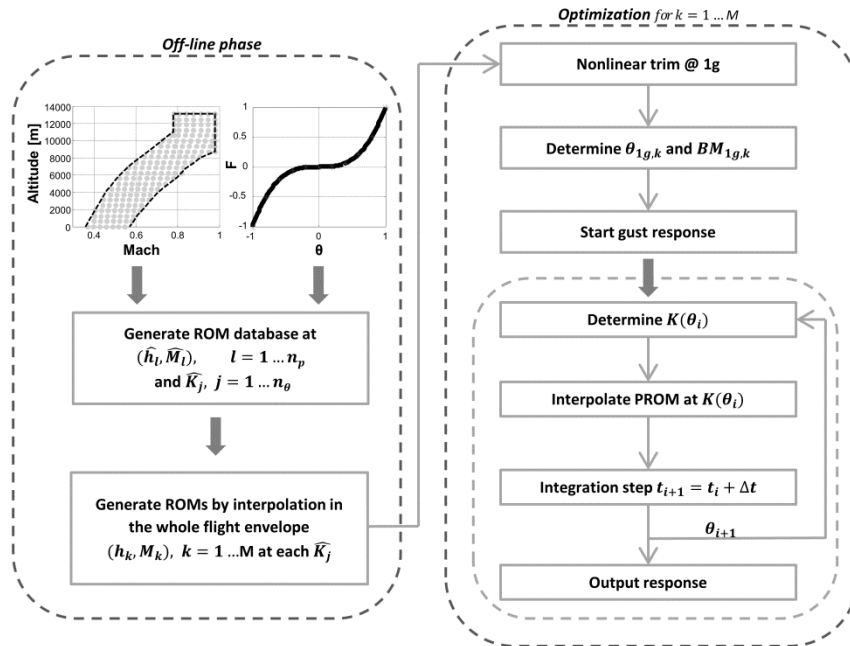


Figure 3. Flowchart of the wing tip optimization procedure.

The advantage of using the PROM methodology is twofold: a complete sweep of the flight envelope and the identification of the worst-case gust for each wing section can be rapidly performed without the need of generating

and using a new FOM at each flight condition, but simply interpolating the database of ROMs generated off-line, and the same reduction and interpolation procedure is used to sample the linearized equivalent stiffness, generate a database of sub-linear ROMs and carry out the nonlinear trim and gust response in a piecewise-linear manner. For the present case, the ROMs database has been created taking 16 points in the flight envelope and 8 points to discretize the stiffness curve. As an example of the substantial saving in computational time, a single nonlinear trim and gust response to ten gust lengths using the ROM requires just 9.5% of the FOM time. The estimated speed-up factor for the complete optimization run exceeds 30.

### Results

The reference aircraft for the wing tip device application is the same used by Ricci et al.<sup>14</sup>, representing a modern narrow-body airliner. The structural model is a FE stick beam model with lumped masses whereas for the aerodynamics the DLM is used. Both the structural and aerodynamic models, shown in Figure 4, are created in Nastran with the publicly available software NeoCASS<sup>27</sup>. The wing tip device increases the wing span by 10% and the attachment element is located at 24% of the root chord with its axis perpendicular to the airstream.

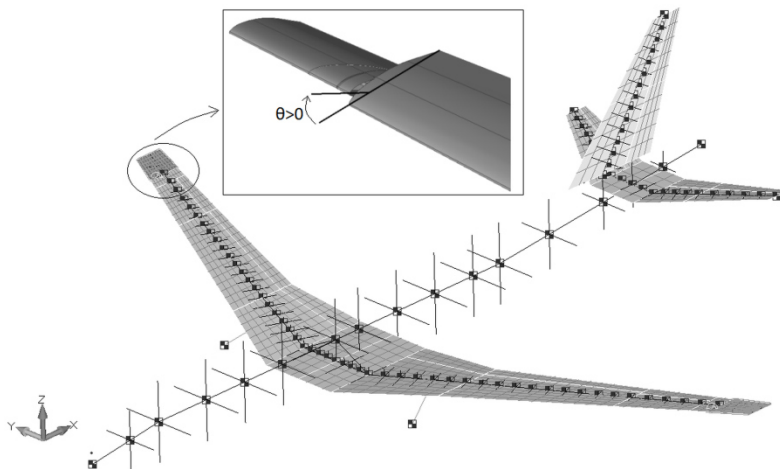


**Figure 4.** Structural and aerodynamic mesh of the reference aircraft and definition of wing tip rotation  $\theta$ .

The optimization is performed via a Multi-Objective Genetic Algorithm<sup>28</sup>. Lower and upper bounds are imposed on the stiffness coefficients (Table 1), as well as a lower bound on the linearized equivalent stiffness. Because the system is nonlinear, a classical p-k flutter analysis cannot be performed, therefore freedom from flutter is ensured by

checking if any of the model coordinates, monitored in the output vector  $\mathbf{y}$ , tends to diverge during the gust response.

The results of the optimizer are presented in Figure 5, which reports the Pareto front and the individuals' distribution. The Pareto-optimal solutions show a greater variability in the misalignment objective function whereas the load alleviation is less sensitive to the stiffness coefficients. The point chosen on the Pareto front is highlighted in Figure 5 and reported in Table 1, compared to the optimized linear design (coefficients normalized to the linear stiffness equal to 33000 Nm/rad<sup>14</sup>). The linear stiffness is increased almost to its upper bound, basically to limit the cruise misalignment. This finding is expected as in cruise, due to the lower lift acting on the wing, the wing tip operates around  $\theta = 0$  deg where the stiffness curve is dominated by the linear term. As the aerodynamic load increases due to a gust encounter, the wing tip deflects and operates in the nonlinear region. Since a more flexible device is more effective in alleviating the loads, the optimal solution features a negative nonlinear stiffness coefficient, i.e. a softening effect. From a practical point of view, a softening effect can occur in a structural element undergoing buckling<sup>3</sup>.

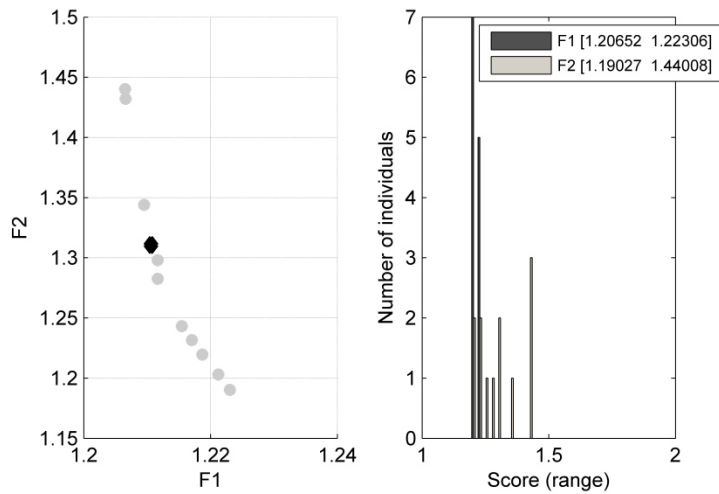


**Figure 5.** Optimization results, Pareto front (left) and score histogram (right).

**Table 1.** Optimized stiffness coefficients, linear vs. nonlinear, and lower and upper bounds.

| Stiffness coefficients | Linear | Nonlinear | LB  | UB  |
|------------------------|--------|-----------|-----|-----|
| $K_0$                  | 1      | 1.1935    | 0.8 | 1.2 |
| $K_{nl}$               | --     | -0.6399   | -3  | 1   |

To illustrate the approach, the time history of the incremental bending moment due to the worst-case positive gust at two wing sections is shown in Figure 6, for the aircraft equipped with the nonlinear and linear wing tip. The additional flexibility introduced by a nonlinear stiffness achieves a reduction of the maximum and minimum peak loads. This is caused by the increased nose-down deflection of the wing tip with nonlinear stiffness under loads with respect to the linear design (+31% deflection), as shown in Figure 7, which also demonstrates how the linearized equivalent stiffness decreases throughout the gust response thanks to the softening effect.

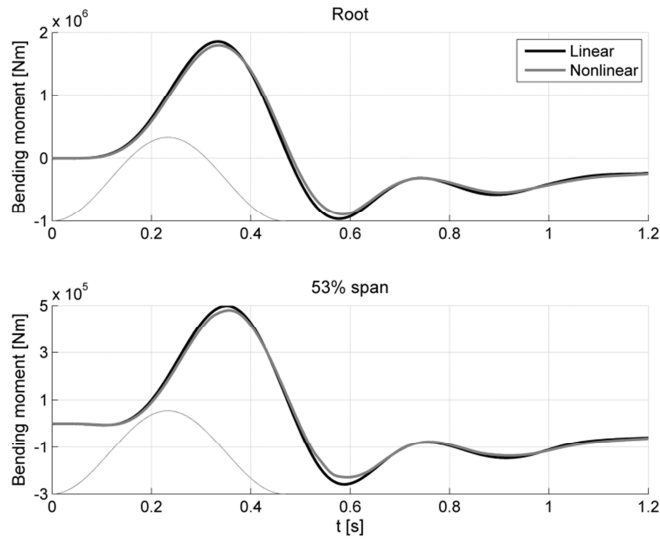


**Figure 6.** Bending moment for worst-case positive gust (shown) at the root and at 53% wingspan, linear vs. nonlinear.



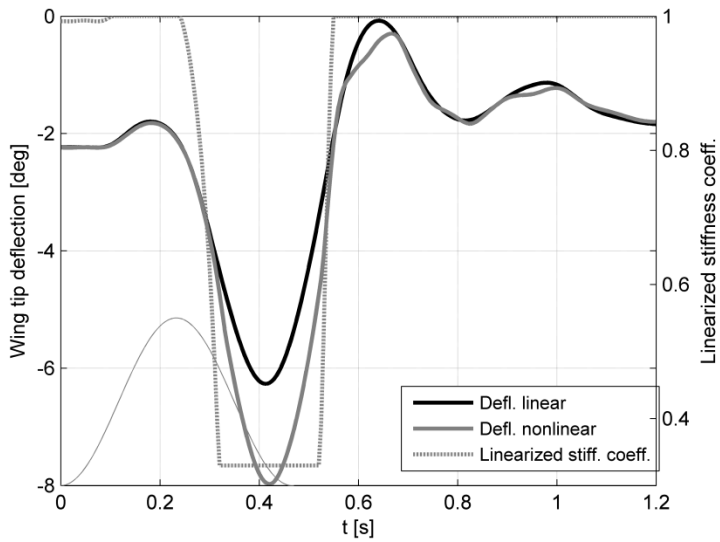


**Figure 7.** Wing tip deflection linear vs. nonlinear and linearized equivalent stiffness for worst-case positive gust (shown).

To assess the behavior of the device in the flight envelope, the ratio of the maximum bending moment of the nonlinear and linear design is presented in Figure 8 at four wing sections. For all flight conditions, the optimized nonlinear device is capable of reducing the loads; the alleviation, though limited at the root, increases towards the outboard wing, an important consideration because this is the area that typically requires structural modification due to a span extension.

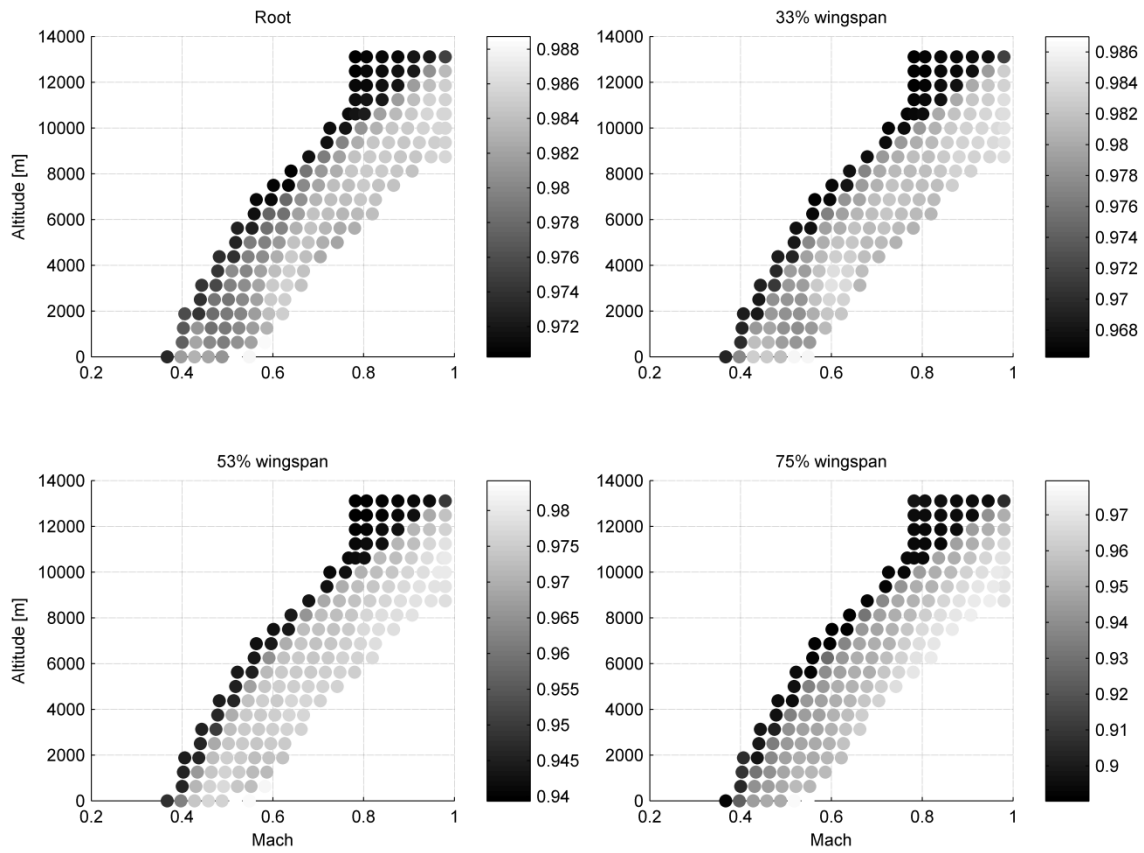


**Figure 8.** Maximum bending moment alleviation (ratio nonlinear/linear) in the flight envelope at four wing sections.

The improvement of the load alleviation capability of the nonlinear design is obtained at the expense of a greater misalignment in cruise, as shown by Figure 9. A detailed aerodynamic assessment is therefore necessary to establish if this offset the reduction of induced drag obtained by the span extension.

Finally the alleviation along the wingspan of the maximum and minimum bending moment for the worst-case gust of each section, i.e. the 1D envelope of the maximum and minimum wing bending moment, is presented in Figure 10 and the critical conditions (Mach, altitude and gust gradient) are summarized in Table 2. The graph reports both the load reduction with respect to the linear wing tip and to a rigid wingspan extension. The device appears to be more effective in reducing the downward bending; nevertheless a good alleviation is obtained, particularly at the outboard wing.

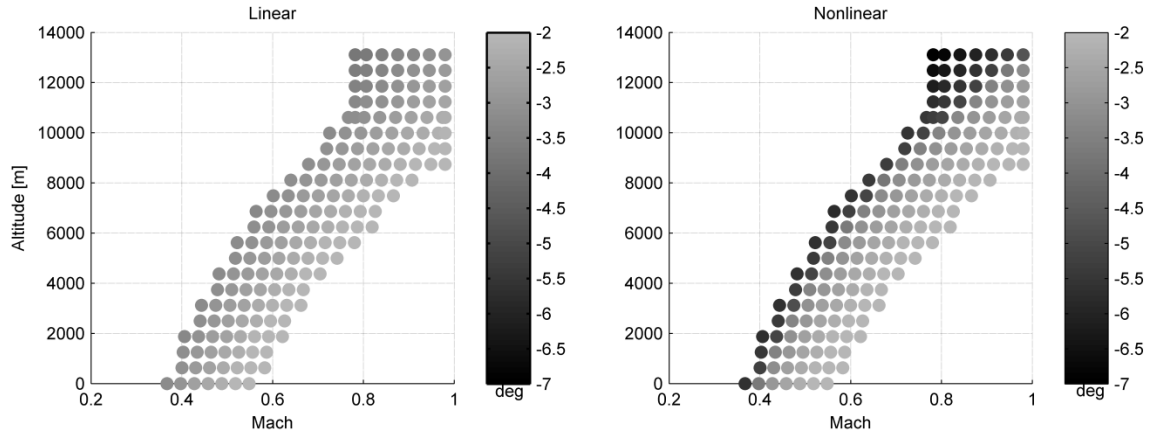


**Figure 9.** Wing tip misalignment at 1g in the flight envelope, linear (left) vs. nonlinear (right).

**Table 2.** Worst-case gust conditions envelope for the wing.

|               | <b>Mach</b> | <b>Altitude (ft)</b> | <b>Gust gradient (ft)</b> |
|---------------|-------------|----------------------|---------------------------|
| <i>Max BM</i> | 0.37        | 0                    | 172                       |
|               | 0.37        | 0                    | 208                       |
|               | 0.43        | 0                    | 172                       |
|               | 0.46        | 0                    | 172                       |
|               | 0.49        | 0                    | 208                       |
| <i>Min BM</i> | 0.49        | 0                    | 208                       |
|               | 0.55        | 2048                 | 208                       |
|               | 0.55        | 2048                 | 244                       |
|               | 0.55        | 2048                 | 279                       |

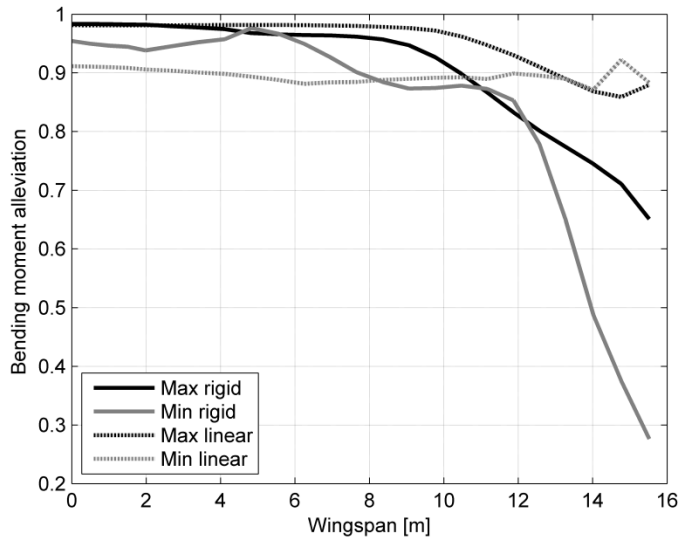


**Figure 10.** Worst gust max/min bending moment alleviation along the wingspan with respect to linear and rigid wing tip.

## Conclusions

In this paper, an efficient methodology for the simulation of aeroelastic systems with concentrated structural nonlinearities has been proposed. The technique relies on the standard linear aeroelastic tools still commonly employed in the industry and performs the simulation in time-domain of a nonlinear aeroelastic system in a piecewise-linear fashion, switching between sub-linear systems according to the current configuration of the states. The efficiency of the procedure is greatly improved by applying a PMOR framework: a database of small yet accurate ROMs is generated in an off-line phase by balanced truncation for few selected flight conditions and few values of the nonlinear property linearized around a specific operating point. During the integration the sub-linear systems are created simply by interpolating the state-space matrices from this database.

The methodology is applied to study the behaviour of a passive wing tip device for load alleviation with a nonlinear stiffness, compared to a previous work where a linear design of the same device was introduced. A multi-objective optimization is carried out to tune the nonlinear stiffness subject to load alleviation and aerodynamic objectives in the whole flight envelope, showing the efficiency of the proposed method which achieves an estimated speed-up factor of 30 compared to a FOM optimization approach.

## Acknowledgements

This work is supported by the European Commission (EC FP7) under the Marie Curie European Industrial Doctorate Training Network ALPES (Aircraft Loads Prediction using Enhanced Simulation – Grant Agreement No. 607911) and the Royal Academy of Engineering.

## References

1. Henshaw MJ, Badcock KJ, Vio GA, Allen AM, Chamberlain J, Kaynes I et al. Non-linear aeroelastic prediction for aircraft applications. *Prog Aerosp Sci* 2007; 43(4-6): 65-137.
2. Dowell E, Edwards J and Strganac TW. Nonlinear aeroelasticity. *J Aircr* 2003; 40(5): 857-874.
3. Lee BHK, Price SJ and Wong YS. Nonlinear aeroelastic analysis of airfoil: bifurcation and chaos. *Prog Aerosp Sci* 1999; 35(3): 205-334.
4. Xiang J, Yan Y and Li D. Recent advance in nonlinear aeroelastic analysis and control of the aircraft. *Chin J Aeronaut* 2014; 27(1): 12-22.
5. Arevalo F, Garcia-Fogeda P and Climent H. Nonlinear time-domain structure/aerodynamics coupling with concentrated structural nonlinearities. In: *Proc. of the 27<sup>th</sup> ICAS*, Nice, France, 19-24 September 2010.
6. Bae JS, Yang SM and Lee I. Linear and nonlinear aeroelastic analysis of fighter-type wing with control surface. *J Aircr* 2002; 39(4): 697-708.
7. Silva GHC, Dal Ben Rossetto G and Dimitriadis G. Reduced order analysis of aeroelastic systems with freeplay using an augmented modal basis. *J Aircr*. Epub ahead of print 01 May 2015. DOI: 10.2514/1.C032912.
8. EASA, Certification Specification for Large Aeroplanes CS-25 Amendment 3, September 2007
9. Wright JR and Cooper JE. *Introduction to Aircraft Aeroelasticity and Loads*. 1st ed New York: Wiley 2007.
10. Rewienski M and White J. A trajectory piecewise-linear approach to model order reduction and fast simulation of nonlinear circuits and micromachined devices. *IEEE Trans Comput Aided Des Integr Circuits* 2003; 22(2): 155-170.
11. Brüls O, Duysinx P and Golinval JC. The global modal parameterization for non-linear model order reduction in flexible multibody dynamics. *Int J Numer Methods Eng* 2007; 69(5): 948-977.
12. Chen PC and Sulaeman E. Nonlinear response of aeroservoelastic systems using discrete state-space approach. *AIAA J* 2003; 41(9): 1658-1666.
13. Benner P, Gugercin S and Willcox K. A survey of model reduction methods for parametric systems. Max Planck Institute Magdeburg Preprints, Germany, 14 August 2013.

14. Ricci S, Castellani M and Romanelli G. Multi-fidelity design of aeroelastic wing tip devices. *Proc IMechE Part G: J Aerospace Engineering* 2012; 227(10): 1596-1607.
15. Albano E and Rodden WP. A doublet-lattice method for calculating lift distributions on oscillating surfaces in subsonic flows. *AIAA J* 1969; 7(2): 279-285.
16. Roger KL. Airplane math modeling methods for active control design. AGARD CP-228 1977.
17. Zentner I and Poirion F. Non-smooth modelling of control surfaces featuring a freeplay nonlinearity in aeroelasticity. In: *Proc. of the 48<sup>th</sup> AIAA/ASME/ASCE/AHS/ASC Structures, Structural Dynamics and Materials Conference*, Honolulu, USA, 23-26 April 2007.
18. Karpel M and Wieseman CD. Time simulation of flutter with large stiffness changes *J Aircr* 1994; 31(2): 404-410.
19. Rose T. Using residual vectors in MSC/NASTRAN dynamic analysis to improve accuracy. In: *Proceedings of MSC World Users' Conference*, 1991.
20. Banavara NK and Newsom JR. Framework for aeroservoelastic analyses involving nonlinear actuators. *J Aircr* 2012; 49(3): 774-780.
21. Antoulas AC. An overview of approximation methods for large-scale dynamical systems. *Ann Rev Control* 2005; 29(2): 181-190.
22. Amsallem D and Farhat C. Interpolation method for the adaption of reduced-order models to parameter changes and its application to aeroelasticity. *AIAA J* 2008; 46(7): 1803-1813.
23. Poussot-Vassal C and Roos C. Generation of a reduced-order LPV/LFT model from a set of large-scale MIMO LTI flexible aircraft models. *Control Eng Pract* 2012; 20(9): 919-930.
24. Zimmermann R. A locally parameterized reduced-order model for the linear frequency domain approach to time-accurate computational fluid dynamics. *SIAM J Sci Comput* 2014; 36(3): 508-537.
25. Panzer H, Mohring J, Eid R and Lohmann B. Parametric model order reduction by matrix interpolation, *at-Automatisierungstechnik* 2010; 58(8): 475-484.
26. Castellani M, Lemmens Y and Cooper JE. Parametric reduced order model for rapid prediction of dynamic loads and aeroelastic response with structural nonlinearities. In: *Proc. of the IFASD2015*, St. Petersburg, Russia, 28 June-02 July 2015.
27. Cavagna L, Ricci S and Travaglini L. NeoCASS: an integrated tool for structural sizing, aeroelastic analysis and MDO at conceptual design level. In: *Proc. of the AIAA Atmospheric Flight Mechanics Conference*, Toronto, Canada, 2-5 August 2010.
28. Kalyanmoy D. *Multi-Objective Optimization Using Evolutionary Algorithms*. 1st ed New York: Wiley 2001.

29. Miller S, Vio GA and Cooper JE. Development of an adaptive wing tip device. In: *Proc. of the 50<sup>th</sup> AIAA/ASME/ASCE/AHS/ASC Structures, Structural Dynamics and Materials Conference*, Palm Springs, USA, 4-7 May 2009.
30. Guo S, Li D and Liu Y. Multi-objective optimization of a composite wing subject to strength and aeroelastic constraints. *Proc IMechE Part G: J Aerospace Engineering* 2011; 226(9): 1095-1106.

## Appendix

### Notation

|                   |  |
|-------------------|--|
| $l_a$             | aerodynamic reference length                               |
| $\mathbf{p}$      | vector of parameters of the aeroelastic state-space system |
| $q_\infty$        | dynamic pressure   |
| $\mathbf{q}_h$    | generalized coordinates                                    |
| $s$               | Laplace variable   |
| $t$               | time   |
| $\mathbf{u}_a$    | FEM displacements  |
| $u$               | aeroelastic state-space system input vector                |
| $x_{ae}$          | aeroelastic state-space system states vector               |
| $x_r$             | ROM states vector  |
| $y$               | aeroelastic state-space system output vector               |
| $BM$              | bending moment   |
| $C_{aa}$          | FEM damping matrix   |
| $C_{hh}$          | generalized damping matrix                                 |
| $\mathcal{F}$     | objective function   |
| $\mathbf{F}_{ag}$ | vector of FEM unsteady aerodynamic forces due to gust      |
| $\mathbf{K}_{aa}$ | FEM stiffness matrix                                       |
| $\mathbf{K}_{hh}$ | generalized stiffness matrix                               |
| $K_0$             | linear coefficient of linearized equivalent stiffness      |
| $K_{nl}$          | nonlinear coefficient of linearized equivalent stiffness   |

|                 |  |
|-----------------|--|
| $M_{aa}$        | FEM mass matrix  |
| $M_{hh}$        | generalized mass matrix  |
| MZFW            | Maximum Zero Fuel Weight   |
| $P_k$           | congruence transformation matrix                                   |
| $Q_{aa}$        | matrix of FEM unsteady aerodynamic forces due to structural motion |
| $Q_{hh}$        | matrix of generalized aerodynamic forces due to structural motion  |
| $Q_{hg}$        | vector of generalized aerodynamic forces due to gust               |
| $T_B$           | balanced truncation reduced order basis                            |
| $U_\infty$      | airspeed   |
| $\beta$         | aerodynamic poles of Rational Function Approximation               |
| $\theta$        | wing tip deflection  |
| $\theta_{1g}$   | wing tip misalignment at 1g  |
| $\Delta t$      | integration time step  |
| $\Delta K_{aa}$ | incremental FEM stiffness matrix                                   |
| $\Phi_{ah}$     | generalized basis  |